Carbohydrate Polymers 105 (2014) 222–228

Contents lists available at ScienceDirect

Carbohydrate Polymers

journal homepage: www.elsevier.com/locate/carbpol

Optimization of physical and mechanical properties for chitosan–nanocellulose biocomposites

Danial Dehnad [a], Zahra Emam-Djomeh [b], Habibollah Mirzaei [a], Seid-Mahdi Jafari [a,*], Saeed Dadashi [b]

[a] Department of Food Material and Process Design Engineering, Faculty of Food Science and Technology, Gorgan University of Agricultural Sciences and Natural Resources, Beheshti Avenue, Gorgan, Iran
[b] Department of Food Science and Technology, Faculty of Agriculture Engineering and Technology, College of Agriculture and Natural Resource, University of Tehran, Karaj, Iran

ARTICLE INFO

Article history:
Received 5 December 2013
Received in revised form 26 January 2014
Accepted 28 January 2014
Available online 5 February 2014

Keywords:
Carbohydrate polymers
Response surface method
Plasticizer
Nanoparticle
Biodegradable films

ABSTRACT

Chitosan (CHT) is a biodegradable compound and has excellent performance in forming films; on the other hand, nanocellulose (NCL) crystals have low densities and are less expensive than other nanofillers. A novel and simple method was applied to develop CHT–NCL nanocomposite (NCP) from CHT powder of high molecular weight and NCL particles having two dimensions in nanoscale; a rotor stator and an ultrasound device were used to separate different nanolayers from each other and facilitate their dispersion into polymer matrix. The optimized NCP indicated superior mechanical properties compared with some synthetic films; approximate values of 47% elongation-at-break, 245 MPa tensile strength and 4430 MPa Young's modulus were achieved. Water vapour permeability (WVP) value of the NCP was at optimal level of 0.23×10^{-11} (g/m s Pa) which was much less than the most biofilms' WVP values. FESEM analyses revealed that high concentrations of CHT and NCL composed inter-connected structures justifying high elongation capability of CHT–NCL NCP.

1. Introduction

Chitosan (CHT), the cationic (1–4)-2-amino-2-deoxy-β-D-glucan, is industrially produced in various quality grades from chitin, the second most abundant polysaccharide in nature (Muzzarelli et al., 2012; Muzzarelli, 2012; Tome et al., 2013). CHT is a non-toxic and biodegradable compound and has excellent performance in forming films (Hardy, Hubert, Macquarrie, & Wilson, 2004). Molecular weight of CHT deeply affects the permeability, mechanical and thermal properties of the obtained film (Butler, Vergano, Testin, Bunn, & Wiles, 1996). CHT films have moderate water vapour permeabilities and exhibit good barrier properties against oxygen permeation (Rudrapatnam & Farooqahrned, 2003).

Cellulose, as the most abundant polymer in the environment, regards as one of the most important elements in the plant structures and guarantees the integrity of cellular structure (Righi et al., 2011). Different cellulose derivations with various applications could be obtained by physicochemical treatments on cellulose; since the aim of treatment application is grinding the long chains of cellulose polymers, hydrolysis process is applied on cellulose microfibrils and then chemical compounds and impurities are removed by washing and residuals are treated by spray drying process (Dadashi, 2011). Obtained crystals have low densities, high elongation moduli and tensile strengths (Klemm, Heublein, & Fink, 2005); besides, they have high biodegradability rates and are less expensive than other nanofillers (Hansson et al., 2013). This highlights their suitability to be applied as nano-reinforcer materials in biodegradable packaging.

Nanocomposites (NCPs) are novel polymer matrices which have been incorporated by nanoparticles (NPs) having at least one dimension in nanoscale (Petersson & Oksman, 2006). Cellulosic nanocomposites are usually used to achieve excellent strength properties (Mikkonen et al., 2011). Dadashi (2011) evaluated the effect of three different levels of the current nanocellulose (NCL) (3, 5 and 7%) on poly lactic acid matrix. Since NCL, as a polysaccharide and hydrophilic compound, is in fibrous state and its dimensions are greater than counterparts of other NPs, it was recommended to be used as a reinforcement constituent in such a way that it won't change the matrix context. They suggested the level of 3% NCL to obtain less water vapour permeability rates and higher tensile moduli for final films. Khan et al. (2012) reported that incorporation of even 1% (w/w) NCL with 5–10 nm width could significantly increase tensile modulus of CHT film, which was equal to 43% increase compared with control CHT film. Of course, when

* Corresponding author. Tel.: +98 1714426462; fax: +98 1714426462.
E-mail addresses: smjafari@gau.ac.ir, jafarism@hotmail.com (S.-M. Jafari).

0144-8617/$ – see front matter © 2014 Elsevier Ltd. All rights reserved.
http://dx.doi.org/10.1016/j.carbpol.2014.01.094

Table 1
RSM Box–Behnken experimental designfor independent variables.

Std. No. of treatment	CHT level (%w/0.6v)	NCL level (%w/w_{CHT})	GLY level (%v/w_{CHT})
1	1.00	0	60
2	1.30	0	60
3	1.00	2	60
4	1.30	2	60
5	1.00	1	30
6	1.30	1	30
7	1.00	1	90
8	1.30	1	90
9	1.15	0	30
10	1.15	2	30
11	1.15	0	90
12	1.15	2	90
13	1.15	1	60
14	1.15	1	60
15	1.15	1	60

5% NPs was incorporated, tensile strength, tensile modulus and elongation at break reached a plateau; incorporation the higher levels of NCL couldn't improve mentioned parameters, attributed to potential aggregation of NCL particles above the threshold point. Hassan, Hassan, and Oksman (2011) reported that improvement of tensile strength for CHT–NCL NCPs was significant with the incorporation of just 2.5% NCL having 7–24 nm diameters, which was attributed to the formation of percolated/interconnected network of cellulose NPs within CHT matrix. In general, previously prepared chitosan–nanocellulose composites did not show appropriate water vapour permeability or mechanical strength rates to substitute common synthetic polymers. The aim of this research was to apply different types of raw materials to warrant better homogeneity for incorporated NCL particles into CHT matrix in order to improve final diverse properties of nanocomposites. Also, our objective was to obtain the optimized amount considering all factors including the raw material consumption and the properties of final NCPs in order to replace synthetic polymers frequently used in the packaging industry.

2. Material and methods

2.1. Materials

CHT powder, having molecular weight of 600–800 kDa, and cellulose NPs, with 20–50 nm diameters, were purchased from Acros Organics Co., Belgium and Asahi Kasei Corp., Japan, respectively. Absolute acetic acid and glycerol (GLY), sodium chloride, calcium chloride and magnesium nitrate were prepared from Merck Co., Germany.

2.2. Film preparation

Certain amounts of CHT powder (Table 1) were dissolved in 40 mL aqueous solution (1%, v/v) of glacial acetic acid; stirring was conducted at 50 °C and 250 rpm by a heater-stirrer (CB162, Stuart®, UK) for 2 h. In parallel, certain amounts of cellulose NPs (Table 1) were added to 20 mL distilled water and dispersed at the same conditions as CHT for 2 h. Then, the solution was homogenized with a rotor stator (IKA®T25 digital, Ultra-Turrax®, Germany) at 8000 rpm for 15 min and an ultrasound device (TI-H-10, Elma®, Germany) at 35 kHz and 100% power without heating for 30 min. Deaeration was conducted in a thermostat vacuum oven (Croydon, Townson & Mercer Ltd., UK) at 600 mmHg for 1 h without heating. The solutions were casted on the center of glass plates which had 100 cm^2 surface areas and were inside the oven at 37 °C; the required time for film forming was 48 h. The dried films were removed from the plates and placed inside the oven for two further days to evaporate residual solvents completely and finally were placed in hermetic packaging plastics (18 cm × 14 cm; Pollyetilen Co., Iran).

2.3. Physical properties of NCPs

2.3.1. Thickness

Thickness of different films was determined by a digital micrometer (Mitutoyo Company, Japan) to the nearest 0.001 mm. For each sample, 8 random positions around the film were measured and mean value was used for determination of physical and mechanical properties.

2.3.2. Transparency

This was determined by a lux-meter device (Testo 540 pocket sized, UK). For this purpose, its light sensor was located under the light source and the number of received luxes from the source was recorded. Then, in the stable conditions, the samples were placed under the light sensor and received luxes were recorded and reported in terms of the percent and on the basis of two obtained values (Dadashi, Mousavi, Emam, Jomeh, & Oromiehie, 2012). Rates of light illustration were measured from four different directions of the films and mean values were reported.

2.3.3. Moisture content

To carry out this analysis, empty capsules were located in the oven at 110 °C for 1 h to reach the constant weight. Film samples were cut into 3 cm × 1 cm pieces; then, they were placed into the capsules and weighed and finally, the capsules were placed in the oven at 110 °C to reach the constant weight (Ghasemlou, Khaksar, Mardani, Shahnia, & Rashedi, 2013). After cooling in the desiccators, the whole films and capsules were weighed to obtain the dry sample weights. Moisture contents of the films were calculated on the basis of wet weight as follows:

$$MC_{Wb} = \left(\frac{\text{Wet sample weight} - \text{Dry sample weight}}{\text{Wet sample weight}} \times 100\right)$$

2.3.4. Solubility in water

The dried films were then immersed in 50 mL of distilled water for 12 h at 25 °C (Ghasemlou, Khodaiyan, Oromiehie, & Yarmand, 2011). Next, the films were taken out from the water by blotting with filter papers previously dried and weighed to remove the surface adsorbed water. Remaining pieces of films were dried at 110 °C to constant weight (Final dry weight). Solubility in water (WS) was calculated by using the following equation:

$$WS = \left(\frac{\text{Initial dry weight} - \text{Final dry weight}}{\text{Initial dry weight}} \times 100\right)$$

2.3.5. Color

The values were determined by a chromameter (Minolta CR 300 Series, Minolta Camera Co., Ltd., Japan). Measurements were performed by placing the NCP films over the standard white paper: $L^* = 93.49$, $a^* = -0.25$ and $b^* = -0.09$. The CIELab scale was used, L^* (white = 100 and black = 0) and chromaticity parameters of a^* (red = 60 to green = −60) and b^* (yellow = 60 to blue = −60) were measured. For each film, 3 different points were selected (Ojagh, Rezaei, Razavi, & Hosseini, 2010).

2.3.6. Water vapor permeability (WVP)

The WVP test was conducted gravimetrically using ASTM procedure E96-95 (1995). At first, the measurement cells filled with anhydrous calcium chloride desiccant to create a 0% RH storage condition and the surfaces of cells were covered with the films and sealed with molten paraffin. To maintain a 75% RH gradient across

the film at 25 °C, a sodium chloride-saturated solution was used in the desiccator. The RH difference between two sides of the films creates a vapor pressure equal to 1753.55 Pa. The cells were weighted at 2-h intervals during 18 h by a digital balance (GK1203, Sartorius Co., Germany) nearest to the 0.0001. The slope of the weight loss versus time was obtained by linear regression. Water vapor transition rate (WVTR) and water vapor permeability were calculated by the following equations, respectively:

$$\text{WVTR} = \left(\frac{\text{Curve slope}}{\text{Film area}}\right)$$

$$\text{WVP} = \left(\frac{\text{Thickness} \times \text{WVTR}}{\text{Pressure difference}}\right)$$

2.4. Mechanical properties of NCPs

Prepared films were placed on the aluminum foils and maintained for moisture equilibrium in desiccator at 25 °C and 50% RH for 24 h. Saturated magnesium nitrate solution was used to meet required relative humidity. Mechanical properties of the films were measured using a SANTAM Machine (STM-5, SANTAM, Iran) according to the ASTM method D882 (ASTM, 2001); initial grip separation and crosshead speed were set at 50 mm and 5 mm/min, respectively. Tensile strength (TS), elongation-at-break (EB) and Young's modulus (YM) were calculated from Force-Extension curves. EB value was calculated as the ratio of the final length at the point of sample rupture to the initial length of a specimen and expressed as a percentage. TS value was calculated by the following equation:

$$\text{TS} = \frac{\text{Maximum force}}{(\text{Film thickness}) \times (\text{Film width})}$$

2.5. Field emission scanning electron microscope (FESEM)

All the specimens were examined by a FESEM (SU8040, Hitachi, Japan) equipment at an accelerating voltage of 10 kV and magnificence of 1–5 KX.

2.6. Statistical analysis

In this research, Response Surface Method and Box–Behnken design with three independent variables including CHT, NCL and GLY at three levels and three replications at central point were used to study the influence of different concentrations for the raw materials on improvement of the responses (probability level of 0.05). Design-Expert® 6.0.2 software was used for regression analysis and to determine the best fitting models.

3. Results and discussion

3.1. Physical properties of CHT–NCL NCPs

The results have been listed in Table 2. Thickness (TH) of NCPs was varied from 118 to 225 μm, higher than normal thickness of CHT films; the cause of this problem is to apply CHT of much higher molecular weight in comparison with previous researches (Ojagh et al., 2010). Transparency rates of NCPs were in the range of 85–92% indicating high capability of CHT–NCL films to transmit light; since the majority of NPs have smaller dimensions than the wavelength of visual light, it is not expected these particles to create any significant changes in film transparency when their dispersion into the polymer matrix is desirable (Zeng, Yu, Lu, & Paul, 2005). In this research, transparency rates (Table 2) and SEM results from internal structures of the prepared films confirmed this phenomenon.

Moisture content of the NCPs was 13–18%, lower than that (20%) reported by Ojagh et al. (2010) and could show appropriate conditions applied for film drying. Moisture content of the

Table 2
Physical properties of chitosan–nanocellulose composites.

Std. No.	Thickness (mm)	Transparency (%)	Moisture content (%)	Water solubility (%)	L^*	a^*	b^*
1	0.13	91.84	16.86	43.36	69.80	−1.16	6.82
2	0.18	88.92	16.44	40.48	73.18	−2.77	17.84
3	0.14	90.60	15.94	42.76	65.67	−2.14	11.96
4	0.18	89.10	15.11	45.55	68.13	−1.76	9.19
5	0.12	90.78	17.00	29.40	71.60	−1.69	9.00
6	0.16	86.70	17.60	26.46	66.40	−2.13	11.19
7	0.15	90.43	14.02	55.97	73.80	−1.19	7.27
8	0.23	89.01	13.79	55.15	70.06	−1.80	11.49
9	0.17	88.65	17.52	29.86	63.64	−1.90	11.34
10	0.22	88.83	16.44	36.34	67.44	−1.91	12.07
11	0.23	87.50	14.85	54.81	66.09	−2.05	16.38
12	0.19	88.39	14.26	56.52	68.97	−1.73	11.57
13	0.19	87.06	15.04	42.18	68.78	−4.06	22.26
14	0.18	85.47	15.47	41.79	63.73	−4.34	24.37
15	0.16	86.97	16.30	44.74	73.78	−4.30	22.38

Table 3
Prediction of physical and mechanical behaviors for CHT–NCL NCPs by fitting different models with the obtained data.

The best fitted models	Prob > F	Lack of fit	R^2
$TH = 0.03\,(CHT) + 0.01\,(GLY) - 0.03\,(CHT)^2$	0.0295	0.43	91.75
$TP = -1.24\,(CHT) + 2.25\,(CHT)^2 - 1.36\,(NCL)^2$	0.0364	0.55	90.95
$MC_{wb} = -0.49\,(NCL) - 1.46\,(GLY)$	<0.0001	0.83	88.16
$WS = 1.58\,(NCL) + 12.55\,(GLY)$	<0.0001	0.38	96.23
$a^* = -0.28\,(CHT) + 1.24\,(CHT)^2 + 1.04\,(NCL)^2 + 1.30\,(GLY)^2 + 0.50\,(CHT)(NCL)$	0.0001	0.45	99.11
$b^* = 1.83\,(CHT) - 7.33\,(CHT)^2 - 4.22\,(NCL)^2 - 5.49\,(GLY)^2 - 3.45\,(CHT)(NCL)$	0.0007	0.49	98.27
$WVP = 0.06\,(CHT) + 0.06\,(NCL) + 0.20\,(GLY) - 0.14\,(CHT)^2 + 0.11\,(NCL)^2 + 0.03\,(GLY)^2 - 0.14\,(NCL)(GLY)$	0.0006	0.07	98.33
$EB = -7.12\,(CHT) + 6.83\,(NCL) + 9.73\,(CHT)^2 + 17.77\,(NCL)^2$	0.0169	0.40	93.51
$TS = -34.48\,(NCL) - 62.17\,(GLY) + 66\,(GLY)(NCL)$	0.0007	0.25	91.59
$EM = -1.56\,(GLY)$	<0.0001	0.24	88.15

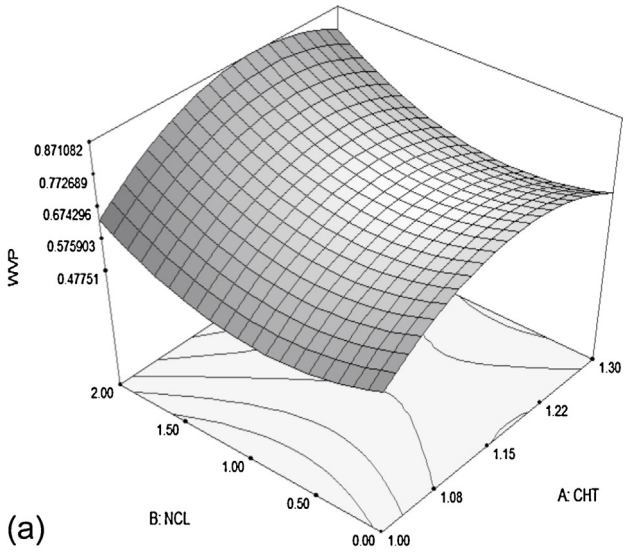

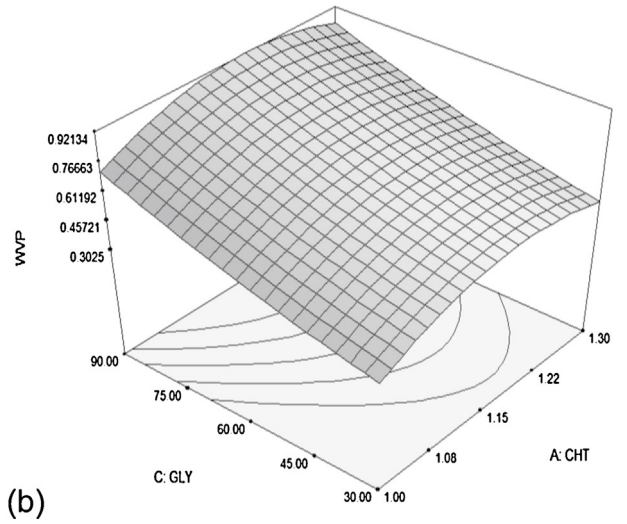

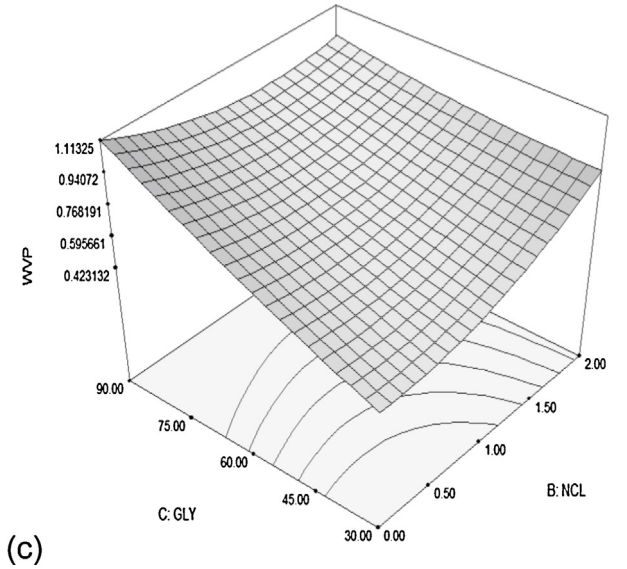

Fig. 1. WVP values of chitosan–nanocellulosenanocomposite as a function of (a) chitosan (CHT) and nanocellulose (NCL), (b) chitosan and glycerol (GLY) and (c) nanocellulose and glycerol.

Table 4
Mechanical properties of CHT–NCL NCPs.

Std. No.	EB (%)	TS (MPa)	EM (MPa)
1	40.33	112.06	3003
2	34.17	67.64	1997
3	70.48	64.43	3418
4	45.39	74.27	1703
5	36.68	152.64	3872
6	17.35	146.82	4421
7	30.78	28.12	947
8	24.41	17.37	716
9	41.59	273.46	3866
10	35.53	24.03	3981
11	22.46	19.74	892
12	41.78	34.33	1129
13	25.22	84.53	3322
14	15.00	97.35	282
15	20.06	66.05	3297

NCPs showed a reverse relationship with applied NPs (Table 3); Fernandes et al. (2010) reported that incorporation of bacterial cellulose with 10–200 nm width caused a slight decrease in moisture content of CHT films. Solubility rates of CHT–NCL NCPs in water were in the range of 26–57%. GLY and NPs were found to be significant effective factors on solubility rates of NCPs (Table 3); sample No. 12, having the highest levels of GLY and NPs, exhibited the highest rate of solubility in water. Generally, water absorption of NCPs depends on the nature of matrix and filler. Water absorption of CHT films increased by incorporating cellulose NPs, in agreement with increment in water vapour permeability rates after NPs addition. Measured values for color parameters of different NCPs have been listed in Table 2. L^* value did not exhibit any relationship with three factors including CHT, NCL and GLY; in other words, all values of this parameter were close to a mean number for various NCPs. Treatments No. 1 and 7, having minimum levels of CHT, deserved the highest rates of a^* value and lowest rates of b^* value, the closest ones to standard values.

Table 5
Comparison of mechanical properties for different (types of) films.

Type of film	Mechanical properties	Reference
CHT–NCL	EB_{max} = 70 (%) TS_{max} = 273 (MPa) EM_{max} = 4.42 (GPa)	Current research
CHT–NCL	EB_{max} = 34.6 (%) TS_{max} = 57.45 (MPa) [a]YM_{max} = 1.63 (GPa)	Azeredo et al. (2010)
CHT–NCL	$Strain_{max}$ = 35 (%) $Stress_{max}$ = 85 (MPa) YM_{max} = 3.75 (GPa)	Fernandes et al. (2009)
CHT–NCL	EB_{max} = 10 (%) TS_{max} = 100 (MPa) YM_{max} = 3.75 (GPa)	Khan et al. (2012)
CHT–NCL	EB_{max} = 25 (%) TS_{max} = 40–110 (MPa) YM_{max} = 6.8 (GPa)	Fernandes et al. (2010)
CHT–NCL	$Strain_{max}$ = 12 (%) TS_{max} = 110 (MPa) EM_{max} = 3.75 (GPa)	De Mesquita, Donnici, Teixeira, & Pereira (2012)
LDPE	EB_{max} = 675 (%) TS_{max} = 31 (MPa) YM_{max} = 0.5 (GPa)	
PP	EB_{max} = 600 (%) TS_{max} = 43 (MPa) YM_{max} = 1.55 (GPa)	Azeredo et al. (2010)
PS	EB_{max} = 2.3 (%) TS_{max} = 70 (MPa) YM_{max} = 3.28 (GPa)	
PVC	EB_{max} = 450 (%) TS_{max} = 55 (MPa) YM_{max} = 0.021 (GPa)	

[a] YM = Young's Modulus.

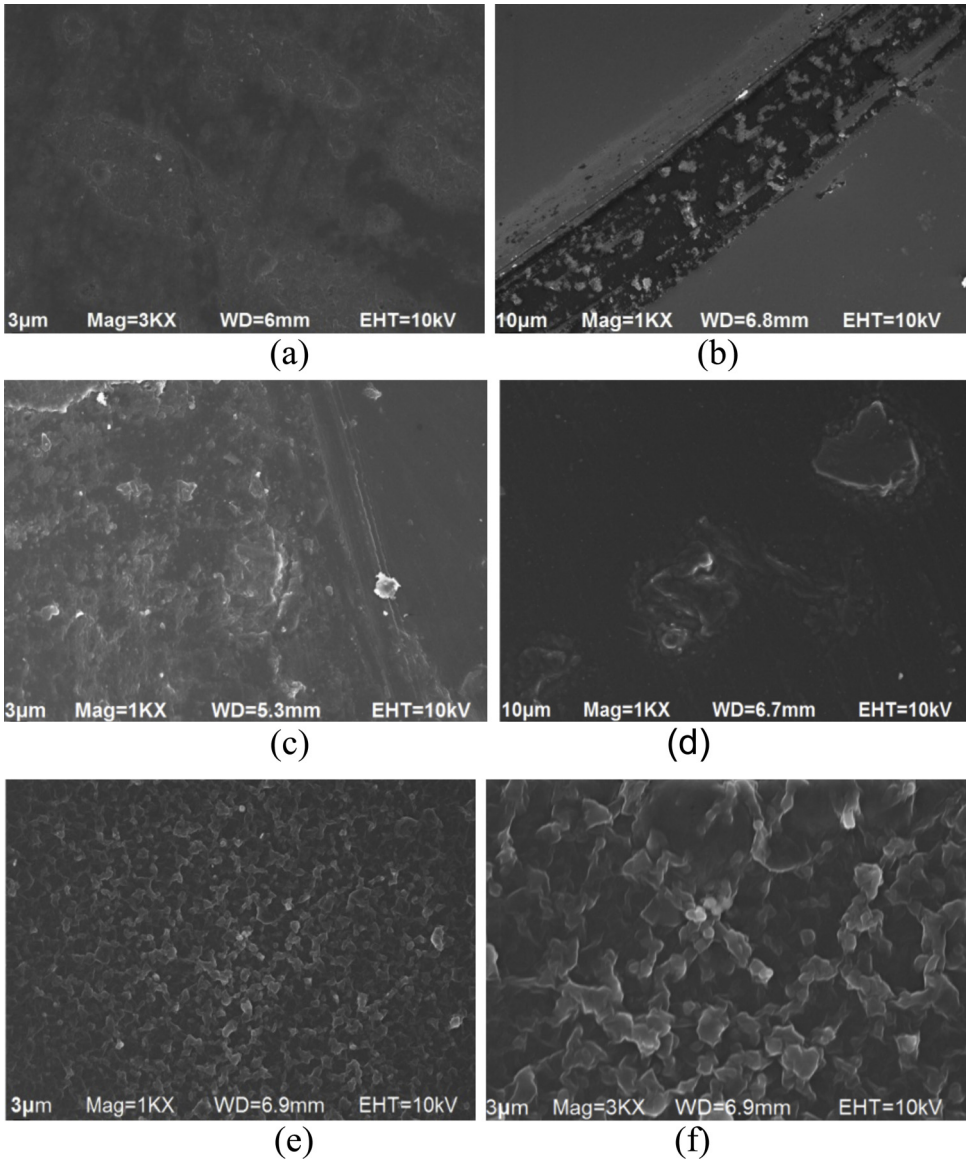

Fig. 2. FESEM micrographs of nanocomposites No. 12 (a), 9 (b), 11 (c), 5 (d) and 4 (e and f).

Water vapour permeability (WVP) is the most studied property of edible films due to its involvement in reactions culminating into food spoilage. WVP and water vapour transmission rate of films are affected by hydrophilic or hydrophobic nature of materials, preparation method, type, level and dispersion quality of additives, voids, cracks or tortuosity into and chains order of polymer (Vasconez, Flores, Campos, Alvarado, & Gerschenson, 2009). Fig. 1 exhibits three-dimensional response surfaces for WVP rates of the NCPs. Sample No. 5, having the minimum levels of CHT and GLY concentrations, showed the lowest rate of WVP. Decreasing GLY concentration from 90 to 30% decreased WVP values, reflecting hygroscopic nature of substance. This response stood for the highest degree of dependence upon the variables; it exhibited direct relationship with the first power of CHT, NCL and GLY and second power of NCL and reverse relationship with the second power of CHT or NCL-GLY interaction (Table 3). Petersson and Oksman (2006) used NCL as a reinforcement agent for poly lactic acid matrix and reported WVP increased along with incorporating particles, attributed to the hydrophilic nature and big particle size of incorporated nanocelllulose.

Much less WVP values were obtained for the current NCPs in comparison with normal biofilms or previously-reported CHT–NCL NCPs; minimum WVP values of approximately 8.1, 75.23, 19.68, 53.24 and 22.06 ($\times 10^{-11}$ g/m s Pa) have been reported for alginate, whey protein isolate/sodium dodecyl sulphate, gelatine, pea starch and hydroxypropyl methylcellulose, respectively (Azeredo et al., 2010).

3.2. Mechanical properties of CHT–NCL NCPs

The results have been listed in Table 4. Increasing NCL level incorporated into CHT films from 0 to 2 could increase elongation at break by 14.6–30.2%. This could be relevant to two factors: (1) proper connections between polymer-nanocrystals (2) efficient transfer of involved stress through polymer-NCL layers. In fact, improvement of elongation properties for the film is due to a suitable stress transfer throughout polymer, even distribution of entered stress and minimizing the areas of stress concentrations (Kanagaraj, Varanda, Zhiltsova, Oliveira, & Simoes, 2007). Decreasing GLY level from 90 to 30% caused significantlyan

improvement in NCPs tensile properties. Addition of plasticizer is necessary for the most biopolymer films to overcome film brittleness caused by intense intermolecular forces (Azeredo et al., 2009); plasticizers can decrease these forces, so improving flexibility and elongation properties of films (Forssell, Lahtinen, Lahelin, & Myllarinen, 2002). On the other hand, plasticizers decrease crystallinity rate of biopolymer films and result in decreasing strength and module values of NCPs (Bangyekan, Aht-Ong, & Srikulkit, 2006). Quadratic model for elongation at break, two factor interactions for tensile strength and linear model for elastic modulus deserved the highest fitting indexes (Table 4).

The prepared NCPs exhibited supreme mechanical properties in comparison with other biofilms or previously prepared CHT–NCL NCPs; large differences for mechanical strength between the current NCPs and common synthetic films are noticeable, too (Table 5).

3.3. FESEM results

The surface area of CHT films was flat and smooth indicating appropriate dissolution for CHT powder into acidic solution. In microscopic figures, random direction and balanced dispersion of cellulose nanocrystals into CHT matrix were obvious; this issue indicated proper compatibility between two constituent elements of NCPs films, which resulted in a final homogenized structure and improved mechanical properties for CHT–NCL NCPs (Azeredo et al., 2009).

Fig. 2 shows internal structure of the NCPs. Fig. 2(a), related to NCP No. 12 having 2% NCL and 90% GLY, indicates an appropriate distribution of cellulose NPs into CHT matrix, implying suitable homogenizing method applied in this research. Fig. 2(b), belonging to film No. 9, describes the cross section of CHT film. White spots observed through the microstructures of most NCPs are attributed to natural impurities inside raw CHT powder. Fig. 2(c), which shows internal structure of film No. 11 (pure CHT without NPs), displays these white impurities. It is to be mentioned that NPs were dispersed in a better and more appropriate manner into CHT matrix with increasing CHT and GLY concentrations; contrariwise, NPs distribution was not suitable and was accompanied by some cracks on the polymer context as CHT and GLY levels decreased. As an illustration, when Fig. 2(a) is compared with Fig. 2(d) representing NCP No. 5 (minimal concentrations of CHT and GLY), more even and efficient dispersion of NPs into NCP No. 12 is clarified. FESEM analysis revealed that high concentrations of CHT and NCL composed complex networks and inter-connected structures simplifying water vapour molecules transitions within cross sections and increasing WVP rates; the intricate structure justifies high elongation capability of CHT–NCL NCP, too. Fig. 2(e) and (f), representing internal structure of NCP No. 4 having 1.3 g CHT and 2% NCL, clearly shows those canals throughout the film.

Table 6
Optimization of CHT–NCL nanocomposites' preparation in terms of physical and mechanical responses obtained for the films.

Factor name	Goal	Importance	Optimized value
CHT	Minimize	2	1.00 (%w/0.6v)
NCL	Minimize	2	0.18 (%w/w_{CHT})
GLY	Minimize	1	30 (%v/w_{CHT})
TP	Maximize	1	92.44 (%)
MC	Minimize	1	17.74 (%)
WS	Minimize	3	29.66 (%)
a^*	Maximize	1	−0.42
b^*	Minimize	2	2.00
WVP	Minimize	3	0.23 ($\times 10^{-11}$ g/m S Pa)
EB	Maximize	3	46.80 (%)
TS	Maximize	1	245.05 (MPa)
EM	Maximize	1	4430 (MPa)

3.4. Optimization procedure

If CHT, NCL and GLY are used at 1% (w/0.6 v), 0.18% (w/w_{CHT}) and 30% (w/v) levels to prepare film, it'll give the highest overall desirability of 75% considering all 12 variables and responses (Table 6). For optimized film, the values of some responses such as transparency, a^* value and elastic modulus were at higher amounts than that of treated films and some other responses like WVP and b^* values were at lower rates than the lowest rates of treated ones, interpreting the high overall desirability obtained for the optimized film.

4. Conclusion

Three main drawbacks of biocomposites are their poor water vapor permeability values, unsatisfactory mechanical properties and unacceptable water resistance in comparison with common synthetic films. In contrast, the CHT–NCL NCP deserved suitable bionanocomposite title; water vapor permeability values of the prepared NCPs were in the appropriate range of 0.293–1.072 $\times 10^{-11}$ (g/m s Pa) and maximum amounts of 70% EB, 273.46 TS and 4421 YM were achieved for the NCP. Transparency rates of the prepared NCPs were in the range of 85–92%. As the results showed, water solubility of the NCP films can be controlled by adjusting the concentration of incorporated NCL and the glycerol amount; too high WS values for the NCPs might destroy the quality and consumer desirability of the packaged product. Addition of cellulose nanoparticles to chitosan films decreased moisture content, increased (till 30.2%) elongation-at-break and improved a^* and b^* values for final nanocomposites; reducing glycerol concentration caused a decrease (till 28.7%) in water solubility and water vapour permeability rate and simultaneously increased (till 3.7 GPa) elastic module of the nanocomposite. We found that 1 g chitosan, 0.18% nanocellulose and 30% glycerol led to the highest desirability (75%) for final nanocomposites.

Acknowledgments

It is necessary to appreciate Iran Nanotechnology Initiative Council (INIC) for their financial support. This research was done by cooperation of Gorgan University of Agricultural Sciences and Natural Resources and University of Tehran. All practical stages of this research were performed in Transport Phenomena Laboratory (TPL) at the College of Agriculture and Natural Resource in University of Tehran; we want to give special thanks to the responsible persons.

References

ASTM. (1995). *Standard test methods for water vapour transmission of material.* Philadelphia, PA: American Society for Testing and Materials, Standard E 95-96.

ASTM. (2001). *Standard test method for tensile properties of thin plastic sheeting.* Philadelphia, PA: American Society for Testing and Materials, Standard D882.

Azeredo, H. M. C., Mattoso, L. H. C., Avena-Bustillos, R. J., Filho, G. C., Munford, M. L., Wood, D., et al. (2010). Nanocellulose reinforced chitosan composite films as affected by nanofiller loading and plasticizer content. *Journal of Food Science*, *75*, N1–N7.

Azeredo, H. M. C., Mattoso, L. H. C., Wood, D., Williams, T. G., Bustillos, R. J. A., & McHugh, T. H. (2009). Nanocomposite edible films from mango puree reinforced with cellulose nanofibers. *Journal of Food Science*, *74*, 31–35.

Bangyekan, C., Aht-Ong, D., & Srikulkit, K. (2006). Preparation and properties evaluation of chitosan-coated cassava starch films. *Carbohydrate Polymers*, *63*, 61–71.

Butler, B. L., Vergano, P. J., Testin, R. F., Bunn, J. M., & Wiles, J. L. (1996). Mechanical and barrier properties of edible chitosan films as affected by composition and storage. *Journal of Food Science*, *61*, 953–955.

Dadashi, S. (2011). *The Effect of Adding Nanoparticles on Mechanical and Thermal Properties of PLA Films* (M.S. thesis). Iran: Faculty of Agriculture, University of Tehran.

Dadashi, S., Mousavi, S. M., Emam-Djomeh, Z., Jomeh, D., & Oromiehie, A. (2012). Films based on poly(lactic acid) biopolymer: effect of clay and cellulosic nanoparticles on their physical, mechanical and structural properties. *Iranian Journal of Polymer Science and Technology*, *25*, 127–136.

De Mesquita, J. P., Donnici, C. L., Teixeira, I. F., & Pereira, F. V. (2012). Bio-based nanocomposites obtained through covalent linkage between chitosan and cellulose nanocrystals. *Carbohydrate Polymers*, *90*(1), 210–217.

Fernandes, S. C. M., Freire, C. S. R., Silvestre, A. J. D., Pascoal Neto, C., Gandini, A., Berglund, L. A., et al. (2010). Transparent chitosan films reinforced with a high content of nanofibrillated cellulose. *Carbohydrate Polymers*, *81*, 394–401.

Fernandes, S. C. M., Oliveira, L., Freire, C. S. R., Silvestre, A. J. D., Neto, C. P., Gandini, A., et al. (2009). Novel transparent nanocomposite films based on chitosan and bacterial cellulose. *Green Chemistry*, *11*, 2023–2029.

Forssell, P., Lahtinen, R., Lahelin, M., & Myllarinen, P. (2002). Oxygen permeability of amylase and amylopectin films. *Carbohydrate Polymers*, *47*, 125–129.

Ghasemlou, M., Khaksar, R., Mardani, T., Shahnia, M., & Rashedi, H. (2013). Preparation and investigation of antimicrobial biodegradable edible film based on corn starch. *Iranian Journal of Nutrition Sciences and Food Technology*, *7*, 115–123.

Ghasemlou, M., Khodaiyan, F., Oromiehie, A., & Yarmand, M. S. (2011). Characterization of edible emulsified films with low affinity to water based on kefiran and oleic acid. *International Journal of Biological Macromolules*, *49*, 378–384.

Hansson, S., Trouillet, V., Tischer, T., Goldmann, A. S., Carlmark, A., Barner-Kowollik, C., et al. (2013). Grafting efficiency of synthetic polymers onto biomaterials: A comparative study of grafting-*from* versus grafting-*to*. *Biomacromolecules*, *14*, 64–74.

Hardy, J. J. E., Hubert, S., Macquarrie, D. J., & Wilson, A. J. (2004). Chitosan based heterogeneous crystals for Suzuki and heck reactions. *Green Chemistry*, *6*, 53–56.

Hassan, M., Hassan, E., & Oksman, K. (2011). Effect of pretreatment of bagasse fibers on the properties of chitosan/microfibrillated cellulose nanocomposites. *Journal of Materials Science*, *46*, 1732–1740.

Kanagaraj, S., Varanda, F. R., Zhiltsova, T. V., Oliveira, M. S., & Simoes, J. A. O. (2007). Mechanical properties of high density polyethylene/carbon nanotube composites. *Composites Science and Technology*, *67*, 3071–3077.

Khan, A., Khan, R. A., Salmieri, S., Le Tien, C., Riedl, B., Bouchard, J., et al. (2012). Mechanical and barrier properties of nanocrystalline cellulose reinforced chitosan based nanocomposite films. *Carbohydrate Polymers*, *90*, 1601–1608.

Klemm, D., Heublein, B., & Fink, H. P. (2005). Cellulose: Fascinating biopolymer and sustainable raw material. *Angewandte Chemie International Edition*, *44*, 3358–3393.

Mikkonen, K., Stevanic, J., Joly, C., Dole, P., Pirkkalainen, K., Serimaa, R., et al. (2011). Composite films from spruce galactoglucomannans with microfibrillated spruce wood cellulose. *Cellulose*, *18*, 713–726.

Muzzarelli, R. A. A. (2012). Nanochitins and nanochitosans, paving the way to eco-friendly and energy-saving exploitation of marine resources. *Polymer Science: A Comprehensive Reference*, *10*, 153–164.

Muzzarelli, R. A. A., Boudrant, J., Meyer, D., Manno, N., DeMarchis, M., & Paoletti, M. G. (2012). A tribute to Henri Braconnot, precursor of the carbohydrate polymers science, on the chitin bicentennial. *Carbohydrate Polymers*, *87*, 995–1012.

Ojagh, S. M., Rezaei, M., Razavi, S. H., & Hosseini, S. M. H. (2010). Development and evaluation of a novel biodegradable film made from chitosan and cinnamon essential oil with low affinity toward water. *Food Chemistry*, *122*, 161–166.

Petersson, L., & Oksman, K. (2006). Biopolymer based nanocomposites: Comparing layered silicates and microcrystalline cellulose as nanoreinforcement. *Composite Science and Technology*, *66*, 2187–2196.

Righi, S., Morfino, A., Galletti, P., Samori, C., Tugnoli, A., & Stramigioli, C. (2011). Comparative cradle-to-gate life cycle assessments of cellulose dissolution with 1-butyl-3-methylimidazolium chloride and N-methyl-morpholine-N-oxide. *Green Chemistry*, *13*, 367–375.

Rudrapatnam, N. T., & Farooqahrned, S. K. (2003). Chitin – The undisputed biomolecule of great potential. *Critical Review in Food Science and Nutrition*, *43*, 61–87.

Tome, L. C., Fernandes, S. C. M., Perez, D. S., Sadocco, P., Silvestre, A. J. D., Neto, C. P., et al. (2013). The role of nanocellulose fibers, starch and chitosan on multi-polysaccharide based films. *Cellulose*, *20*(4), 1807–1818.

Vasconez, M. B., Flores, S. K., Campos, C. A., Alvarado, J., & Gerschenson, L. N. (2009). Antimicrobial activity and physical properties of chitosan–tapioca starch based edible films and coatings. *Food Research International*, *42*, 762–769.

Zeng, Q. H., Yu, A. B., Lu, G. Q. M., & Paul, D. R. (2005). Clay-based polymer nanocomposites: Research and commercial development. *Journal of Nanoscience and Nanotechnology*, *5*, 1574–1592.